# Chapter 20

# Basic Principles of Radio Astrometry


## Alain Baudry[1] & Roberto Neri[2]

**baudry@observ.u-bordeaux.fr & neri@iram.fr**

[1] Observatoire de Bordeaux, BP 89, F-33270 Floirac, France

[2] IRAM, 300 rue de la piscine, F-38406 Saint-Martin-d'Hères, France


## 20.1 Introduction and Basic Formalism

Modern astrometry aims at improving our knowledge of celestial body positions, motions and distances to a high accuracy. The quest for accuracy began in the early days of astronomy and is still continuing in the optical domain with most sophisticated instruments (automated meridian circles, the Hipparcos satellite or future astrometric space missions) as well as in the radio domain (connected-element interferometers and VLBI). New instrumental concepts or calibration procedures and increased sensitivity are essential to measure highly accurate positions of stars and radio sources. Positions accurate to about one thousandth to one tenth of an arcsecond have now been obtained for hundreds of radio sources and for about 100 000 to one million stars in the Hipparcos and Tycho catalogues respectively.

In this lecture we are concerned with some basic principles of position measurements made with synthesis radio telescopes and with the IRAM interferometer in particular. More details on interferometer techniques can be found in the fundamental book of [Thompson et al. 1986]. The impact of VLBI in astrometry and geodesy is not discussed here. (For VLBI techniques see [Sovers et al. 1998].)

We first recall that measuring a position is a minimum prerequisite to the understanding of the physics of many objects. One example may be given for illustration. To valuably discuss the excitation of compact or masing molecular line sources observed in the direction of late-type stars and HII regions sub-arcsecond position measurements are required. This is because the inner layers of circumstellar envelopes around late-type stars have sizes of order one arcsecond or less and because several compact HII regions have sizes of one to a few arcseconds only. Position information is crucial to discuss not only the respective

importance of radiative and collisional pumping in these line sources but also the physical asssociation with the underlying central object.

The output of an interferometer per unit bandwidth at the observing wavelength $\lambda$ is proportional to the quantity

$$R = \int A(\vec{k}) I(\vec{k}) \cos(2\pi \vec{\mathcal{B}}.\vec{k}/\lambda) d\Omega \tag{20.1}$$

where $\vec{k}$ is the unit vector toward the observed source, $A$ is the effective antenna aperture, $I$ the source brightness, and $\vec{\mathcal{B}}$ the baseline vector of the interferometer. For an extended source one refers the observations to the reference direction $\vec{k}_0$ and supposing that the radiation comes from a small portion of the sky we have $\vec{k} = \vec{k}_0 + \vec{\sigma}$ where $\vec{\sigma}$ is the position vector describing the source coordinates. (Since both $\vec{k}_0$ and $\vec{k}$ are unit vectors we obtain $\vec{k}_0.\vec{\sigma} = 0$.) The interferometer output is given by

$$R = V \cos(2\pi \vec{\mathcal{B}}.\vec{k}_0/\lambda + \Psi) \tag{20.2}$$

where

$$V \exp(i\Psi) = \int A(\vec{\sigma}) I(\vec{\sigma}) \exp(i 2\pi \vec{b}.\vec{\sigma}) d\Omega \tag{20.3}$$

is the complex source visibility and $\vec{b}(u,v)$ is the baseline vector projected on a plane normal to the tracked direction. The exact definition of the baseline coordinates $u$ and $v$ is given in Section 20.3.

The astrometry domain corresponds to those cases where the source visibility amplitude is equal to 1 (point-like sources) and the phase provides the source position information.

## 20.2 The Phase Equation

The most important measurement for radio astrometry is that of the actual fringe phase of a connected-element interferometer (or similarly the group delay in VLBI). Let $\theta$ be the angle between the reference direction and the meridian plane of a given interferometer baseline. The phase is then defined by

$$\phi_r = 2\pi \mathcal{B} \sin(\theta)/\lambda \tag{20.4}$$

If the point-like source of interest is offset by $\Delta\theta$ from the reference direction the total phase is

$$\phi = 2\pi \mathcal{B} \sin(\theta + \Delta\theta)/\lambda \simeq \phi_r + 2\pi \mathcal{B} \cos(\theta) \Delta\theta/\lambda \tag{20.5}$$

It is thus clear that measuring an angle or an offset position on the celestial sphere becomes possible only when all phase calibration problems have been understood and solved.

Accounting for uncertainties in the baseline and source position vectors the actual phase is

$$\phi = 2\pi(\vec{\mathcal{B}} + \delta\vec{\mathcal{B}}).(\vec{k}_0 + \delta\vec{k})/\lambda \tag{20.6}$$

where $\vec{\mathcal{B}}$ is a first approximation of the baseline, $\vec{k}_0$ the tracking direction; $\vec{\mathcal{B}} + \delta\vec{\mathcal{B}}$ and $\vec{k}_0 + \delta\vec{k}$ are the true baseline and source position vectors, respectively. The reference phase is given by

$$\phi_r = 2\pi \vec{\mathcal{B}}.\vec{k}_0/\lambda \tag{20.7}$$

and, neglecting the term involving $\delta\vec{\mathcal{B}}.\delta\vec{k}$, we obtain

$$\phi - \phi_r = 2\pi(\vec{\mathcal{B}}.\delta\vec{k} + \delta\vec{\mathcal{B}}.\vec{k}_0)/\lambda \tag{20.8}$$

We consider all vector projections in the right-handed equatorial system defined by the unit vectors $a_1$ ($H = 6$ h, $\delta = 0$), $a_2$ ($H = 0$ h, $\delta = 0$), $a_3$ ($\delta = 90°$). (Note that this system is not the Cartesian coordinate system used in [Thompson et al. 1986].) $H$ and $\delta$ are the hour angle and declination, respectively. In the

equatorial system the baseline vector $\vec{\mathcal{B}}$ has components $(\mathcal{B}_\infty, \mathcal{B}_\in, \mathcal{B}_\ni)$ and the components of the reference position $\vec{k}_0$ are given by $(\cos(\delta)\sin(H), \cos(\delta)\cos(H), \sin(\delta))$

The two limiting cases $\delta\vec{k} = 0$, and $\delta\vec{\mathcal{B}} = 0$ correspond to those where we either calibrate the baseline or determine the exact source position.

In the first case the source coordinates are perfectly known and by comparing the observed phase $\phi$ with the reference phase $\phi_r$ one determines $\delta\vec{\mathcal{B}}$ and hence the true baseline $\vec{\mathcal{B}} + \delta\vec{\mathcal{B}}$. The reference sources observed for baseline calibration are bright quasars or galactic nuclei whose absolute coordinates are accurately known. The most highly accurate source coordinates are those of the radio sources used to realize by VLBI the International Celestial Reference Frame (ICRF); distribution of coordinate errors are below one milliarcsecond. However, the ICRF catalogue is insufficient for phase and baseline calibrations of millimeter-wave arrays because most sources are not bright enough in the millimeter-wave domain. The IRAM calibration source list is thus a combination of several catalogues of compact radio sources. Today, the Plateau de Bure Interferometer catalogue of calibration sources is based mostly on compact radio sources from the Jodrell Bank – VLA Astrometric Survey (JVAS – [Patnaik et al 1992], [Browne et al. 1998], [Wilkinson et al. 1998]).

## 20.3 Determination of Source Coordinates and Errors

Once the baseline is fully calibrated ($\delta\vec{\mathcal{B}} = 0$) the exact source coordinates are known from the $\delta\vec{k}$ vector components. These components are formally deduced from the differential of $\vec{k}_0$. In the right-handed equatorial system defined in Section 20.2 we obtain

$$\begin{aligned} \delta\vec{k} \;=\; & (-\sin(\delta)\sin(H)\Delta\delta - \cos(\delta)\cos(H)\Delta\alpha, \\ & -\sin(\delta)\cos(H)\Delta\delta + \cos(\delta)\sin(H)\Delta\alpha, \\ & \cos(\delta)\Delta\delta) \end{aligned} \tag{20.9}$$

where $\Delta\alpha$ and $\Delta\delta$ are the right ascension and declination offsets in the equatorial system ($\Delta\alpha = -\Delta H$). The phase difference is then a sinusoid in $H$

$$\frac{(\phi - \phi_r)\lambda}{2\pi} = \vec{\mathcal{B}}.\delta\vec{k} = C_1\sin(H) + C_2\cos(H) + C_3 \tag{20.10}$$

where

$$C_1 = -\mathcal{B}_1\sin(\delta)\Delta\delta + \mathcal{B}_2\cos(\delta)\Delta\alpha \tag{20.11}$$

$$C_2 = -\mathcal{B}_2\sin(\delta)\Delta\delta - \mathcal{B}_1\cos(\delta)\Delta\alpha \tag{20.12}$$

$$C_3 = \mathcal{B}_3\cos(\delta)\Delta\delta + \phi_{\rm ins} \tag{20.13}$$

and $C_3$ contains the instrumental phase $\phi_{\rm ins}$.

Measurement of the phase at time intervals spanning a broad hour angle interval allows us to determine the three unknowns $C_1$, $C_2$, and $C_3$, and hence $\Delta\alpha$ and $\Delta\delta$ and the exact source position. Note that for sources close to the equator, $C_1$ and $C_2$ alone cannot accurately give $\Delta\delta$. In the latter case, $C_3$ must be determined in order to obtain $\Delta\delta$; this requires to accurately know the instrumental phase and that the baseline is not strictly oriented along the E-W direction (in which case there is no polar baseline component).

A synthesis array with several, well calibrated, baseline orientations is thus a powerful instrument to determine $\delta\vec{k}$. In practice, a least-squares analysis is used to derive the unknowns $\Delta\alpha$ and $\Delta\delta$ from the measurements of many observed phases $\phi_i$ (at hour angle $H_i$) relative to the expected phase $\phi_r$. This is obtained by minimizing the quantity $\Sigma(\Delta\phi_i' - (C_1\sin(H_i) + C_2\cos(H_i) + C_3))^2$ with respect to $C_1$, $C_2$, and $C_3$ where $\Delta\phi_i' = (\phi_i - \phi_r)\lambda/2\pi$. A complete analysis should give the variance of the derived quantities $\Delta\alpha$ and $\Delta\delta$ as well as the correlation coefficient.

Of course we could solve for the exact source coordinates and baseline components simultaneously. However, measuring the baseline components requires to observe several quasars widely separated on the sky. At mm wavelengths where atmospheric phase noise is dominant this is best done in a rather short

observing session whereas the source position measurements of often weak sources are better determined with long hour angle coverage. This is why baseline calibration is usually made in separate sessions with mm-wave connected-element arrays.

The equation giving the source coordinates can be reformulated in a more compact manner by using the components $u$ and $v$ of the baseline projected in a plane normal to the reference direction. With $v$ directed toward the north and $u$ toward the east, the phase difference is given by

$$(\phi - \phi_r) = 2\pi(u\cos(\delta)\Delta\alpha + v\Delta\delta) \tag{20.14}$$

Comparing this formulation to the sinusoidal form of the phase difference we obtain

$$u = (-\mathcal{B}_1\cos(H) + \mathcal{B}_2\sin(H))/\lambda \tag{20.15}$$

$$v = (\mathcal{B}_3\cos(\delta) - \sin(\delta)(\mathcal{B}_1\sin(H) + \mathcal{B}_2\cos(H)))/\lambda \tag{20.16}$$

Transforming the $\mathcal{B}_{1,2,3}$ into a system where the baseline is defined by its length $\mathcal{B} = (\mathcal{B}_1^2 + \mathcal{B}_2^2 + \mathcal{B}_3^2)^{0.5}$ and the declination $d$ and hour angle $h$ of the baseline vector (defined as intersecting the northern hemisphere) we obtain

$$\mathcal{B}_1 = \mathcal{B}\cos(d)\sin(h), \mathcal{B}_2 = \mathcal{B}\cos(d)\cos(h), \mathcal{B}_3 = \mathcal{B}\sin(d) \tag{20.17}$$

and

$$u = (\cos(d)\sin(H-h))\mathcal{B}/\lambda \tag{20.18}$$

$$v = (\cos(\delta)\sin(d) - \sin(\delta)\cos(d)\cos(H-h))\mathcal{B}/\lambda$$

which shows that the locus of the projected baseline vector is an ellipse.

In order to derive the unknowns $\Delta\alpha$ and $\Delta\delta$ the least-squares analysis of the phase data is now performed using the components $u_i, v_i$ derived at hour angle $H_i$. In the interesting case where the phase noise of each phase sample is constant (this occurs when the thermal noise dominates and when the atmospheric phase noise is "frozen") one can show that the error in the coordinates takes a simple form. For a single baseline and for relatively high declination sources the position error is approximated by the equation

$$\sigma_{\alpha,\delta} = \Delta\theta \simeq \sigma_\phi/(2\pi\sqrt{n_p}(\mathcal{B}/\lambda)) \tag{20.19}$$

where $\sigma_\phi$ is the phase noise and $n_p$ the number of individual phase measurements. This result implies (as expected a priori) that lower formal uncertainties are obtained with longer observing times and narrower synthesized beams. Of course the position measurements are improved with several independent interferometer baselines; the precision improves as the inverse of the square root of $n(n-1)/2$ for $n$ antennas in the array.

We have shown that for a well calibrated interferometer the least-squares fit analysis of the phase in the $(u, v)$ plane can give accurate source coordinates. However, the exact source position could also be obtained in the Fourier transform plane by searching for the coordinates of the maximum brightness temperature in the source map. The results given by this method should of course be identical to those obtained in the $(u, v)$ plane although the sensitivity to the data noise can be different.

Finally, it is interesting to remind that the polar component of the baseline does not appear in the equation of the fringe frequency which is deduced from the time derivative of the phase. There is thus less information in the fringe frequency than in the phase.

## 20.4 Accurate Position Measurements with the IRAM Interferometer

Let us start with two general and simple remarks. First, the phase equation in Section 20.2 or the least-square analysis of the $uv$ data in Section 20.3 show that higher position accuracy is achieved for smaller values of the fringe spacing $\lambda/\mathcal{B}$. Thus, for astrometry it is desirable to use long baselines and/or to go to

short wavelengths. However, the latter case implies that the phases are more difficult to calibrate especially at mm wavelengths where the atmospheric phase fluctuations increase with long baselines. Second, sensitivity is always important in radio astrometry. For a point-like or compact source the sensitivity of the array varies directly as $D^2(n(n-1))^{0.5}$ where $D$ is the antenna diameter and $n$ the number of antennas. Thus, the detection speed varies as $D^4 n(n-1)$ and big antennas are clearly advantageous [Baudry 1996].

Comparison of the IRAM 5-element array with one of its competitors, the Owens Valley Radio Observatory array (OVRO) with 6×10.4 m, gives a ratio of detection speed of 1 over 0.36 at 3 mm and 1 over 0.65 at 1.3 mm in favour of the Plateau de Bure array (see Table 1 below where the two entries correspond to 3 mm and 1 mm; system temperatures have been adopted according to advertised array specifications [June 2000]; sensitivity and speed are defined in Table 1). (Note also that the sixth antenna in the Bure array will increase its detection speed by 50%.) For comparison we include in Table 1 the BIMA array located in California and the Nobeyama array in Japan (NMA). In addition, it is interesting to note that the large dishes of the IRAM array are well adapted to quick baseline and phase calibrations; this is another clear advantage of the IRAM interferometer in astrometric observations.

**Table 1. Comparison of Sensitivity and Speed of mm-wave Interferometers**

| | BIMA | | IRAM | | NMA | | OVRO | |
|---|---|---|---|---|---|---|---|---|
| Antennas | 9 | | 5 | | 6 | | 6 | |
| Baseline (m) | 2000 | | 400 | | 400 | | 480 | |
| Sensitivity | 0.31 | 0.26 | 1.00 | 1.00 | 0.42 | 0.06 | 0.36 | 0.65 |
| Speed | 0.10 | 0.07 | 1.00 | 1.00 | 0.18 | — | 0.13 | 0.42 |

$$\text{Sensitivity} = \frac{\eta_A D^2 \sqrt{n(n-1)}}{T_{\rm sys}}, \text{ Speed} = [\frac{\eta_A D^2 \sqrt{n(n-1)}}{T_{\rm sys}}]^2$$

### 20.4.1 Absolute positions

To illustrate the potential of the IRAM array for astrometry we consider here observations of the SiO maser emission associated with evolved late-type stars. Strong maser line sources are excited in the $v = 1, J = 2-1$ transition of SiO at 86 GHz and easily observed with the sensitive IRAM array. Because of molecular energetic requirements (the vibrational state $v = 1$ lies some 2000 K above the ground-state) the SiO molecules must not be located too much above the stellar photosphere. In addition, we know that the inner layers of the shell expanding around the central star have sizes of order one arcsecond or less. Therefore, sub-arcsecond position accuracy is required to locate the SiO sources with respect to the underlying star whose apparent diameter is of order 20-50 milliarcseconds. For absolute position measurements one must primarily:

- select long baselines to synthesize small beamwidths,
- make a highly accurate baseline calibration observing several quasars selected for their small position errors,
- observe at regular intervals two or more quasars (phase calibrators) in the field of each program star in order to determine the instrumental phase and to correct for atmospheric phase fluctuations,
- observe the program star over a long hour angle interval, and use the best estimate of the stellar coordinates (corrected for proper motion).

Our first accurate radio position measurements of SiO masers in stars and Orion were performed with the IRAM array in 1991/1992. We outline below some important features of these observations [Baudry et al. 1994]. We used the longest E-W baseline available at that time, about 300 m, thus achieving beams of order 1.5 to 2 arcseconds. The RF bandpass calibrations were made accurately using strong quasars only. To monitor the variable atmosphere above the array and to test the overall phase stability, we observed a minimum of 2 to 3 nearby phase calibrators. Prior to the source position analysis we determined accurate baseline components; for the longest baselines the r.m.s. uncertainties were in the range 0.1 to 0.3 mm. The positions were obtained from least-square fits to the imaginary part of the

calibrated visibilities. (Note that the SiO sources being strong, working in the $(u,v)$ or image planes is equivalent.)

The final position measurement accuracy must include all known sources of uncertainties. We begin with the formal errors related to the data noise. This is due to finite signal to noise ratio (depending of course on the source strength, the total observing time and the general quality of the data); poorly calibrated instrumental phases may also play a role. In our observations of 1991/1992 the formal errors were around 10 to 30 milliarcseconds. Secondly, phase errors arise in proportion with the baseline error $\delta\vec{\mathcal{B}}$ and the offset between the unit vectors pointing toward the stellar source and the nearby phase calibrator. This phase error is $\delta(\phi-\phi_r) = (\delta\vec{\mathcal{B}}.(\vec{k}_{\rm quasar}-\vec{k}_0))2\pi/\lambda$. Typical values are $\delta\mathcal{B} \simeq 0.2$ mm and $\delta k \sim 10^\circ - 20^\circ$ corresponding to phase errors of $3^\circ$ to $7^\circ$, that is to say less than the typical baseline residual phases. A third type of error is introduced by the position uncertainties of the calibrators. This is not important here because the accuracy of the quasar coordinates used during the observations were at the level of one milliarcsecond.

The quadratic addition of all known or measured errors is estimated to be around $0.07''$ to $0.10''$. In fact, to be conservative in our estimate of the position accuracy we measured the positions of nearby quasars using another quasar in the stellar field as the phase calibrator. The position offsets were around $0.1''$ to $0.2''$ depending on the observed stellar fields; we adopted $0.1''$ to $0.2''$ as our final position accuracy of SiO sources. The SiO source coordinates are derived with respect to baseline vectors calibrated against distant quasars. They are thus determined in the quasi-inertial reference frame formed by these quasars.

Finally, it is interesting to remind a useful rule of thumb which one can use for astrometry-type projects with any connected-element array provided that the baselines are well calibrated and the instrumental phase is stable. The position accuracy we may expect from a radio interferometer is of the order of 1/10th of the synthesized beam (1/20th if we are optimistic). This applies to millimeter-wave arrays when the atmospheric fluctuations are well monitored and understood. With baseline lengths around 400 m the IRAM array cannot provide position uncertainties much better than about $0.05 - 0.1''$ at 86 GHz. Extensions to one kilometer would be necessary to obtain a significant progress; the absolute position measurements could then be at the level of 50 milliarcseconds which is the accuracy reached by the best optical meridian circles.

### 20.4.2 Relative Positions and Self-calibration Techniques

We have measured with the IRAM array the absolute position of the SiO emission sources associated with each spectral channel across the entire SiO emission profile. Any spatial structure related to the profile implies different position offsets in the direction of the star. Such a structure with total extent of about 50 milliarcseconds is observed in several late-type stars. This is confirmed by recent VLBI observations of SiO emission in a few stars. VLBI offers very high spatial resolution but poor absolute position measurements in line observations.

The best way to map the relative spatial structure of the SiO emission is to use the phase of one reference feature to map all other features. This spectral self-calibration technique is accurate because all frequency-independent terms are cancelled out. The terms related to the baseline or instrumental phase uncertainties as well as uncalibrated atmospheric effects are similar for all spectral channels and cancel out in channel to channel phase differences. By making the difference

$$(\phi(\nu) - \phi(\nu_{\rm ref}))(\lambda/2\pi) = \vec{\mathcal{B}}.\delta\vec{k}(\nu) - \vec{\mathcal{B}}.\delta\vec{k}(\nu_{ref}) \tag{20.20}$$

where the SiO reference channel is at frequency $\nu_{ref}$ we obtain a phase difference equation whose solution gives the coordinate offsets $\Delta\alpha(\nu)$ and $\Delta\delta(\nu)$ relative to channel $\nu_{ref}$. The main limitation in such self-calibration techniques comes from the thermal noise and the achieved signal to noise ratio SNR. In this case [Reid et al. 1988] showed that the one sigma position uncertainty or angular uncertainty $\Delta\theta$ is approximately given by the equation

$$\Delta\theta = 0.5(\lambda/\mathcal{B})/{\rm SNR} \tag{20.21}$$

Common practice with connected-element arrays shows that selection of a reference channel is not critical; it must be strong in general. Self-calibration proved to be successful with the IRAM array in several stars

and Orion where we have obtained accurate relative maps of SiO emission. Detailed and accurate relative maps were also obtained for the rare isotope $^{29}$SiO emission which is nearly 2 orders of magnitude weaker than that of the main isotope [Baudry et al. 1998]. A relative position accuracy of 2 to 5 milliarcsec was obtained in the Orion spot map of $^{28}$SiO emission (Fig. 20.1).

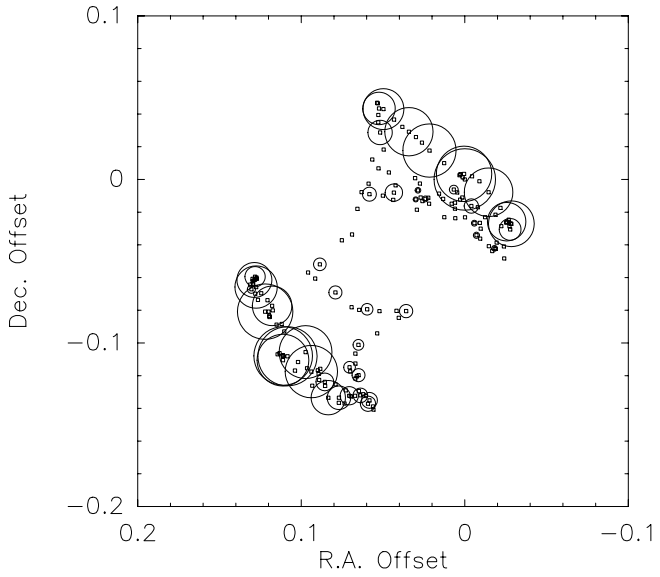


Figure 20.1: Spot map of $^{28}$SiO $v = 1, J = 2 \rightarrow 1$ emission observed on August 1995 in the direction of Orion IRc2 [Baudry et al. 1998]. The right ascension and declination offsets are in arcsec. Each small open square marks the center of an individual channel. The diameter of each circle, given every 3 channels, is proportional to the line intensity. The two main ridge of $^{28}$SiO emission cover $-1 \rightarrow -10$ (southern ridge) and $12 \rightarrow 20$ kms$^{-1}$.

The relative spot maps obtained with connected-element arrays do not give the detailed spatial extent of each individual channel. This would require a spatial resolution of about one milliarcsecond which can only be achieved with VLBI techniques. Note however that VLBI is sensitive to strong emission features while the IRAM array allows detection of very weak emission; thus the two techniques appear to be complementary.

With SiO spatial extents of about 50 milliarcseconds and absolute positions at the level of 0.1 arcsecond it is still difficult to locate the underlying star. We have thus attempted to obtain simultaneously the position of one strong SiO feature relative to the stellar photosphere and the relative positions of the SiO sources using the 1 and 3 mm receivers of the IRAM array. This new dual frequency self-calibration technique is still experimental but seems promising.

## 20.5 Sources of Position Uncertainty

We have given evidence that extended baselines are best for accurate position measurements. In addition, as long as sensitivity is not an issue and that observed sources are not resolved by the array, the outermost stations should always be preferred (Section 20.4). The great asset of the IRAM array is clearly sensitivity coupled with resolving power, although atmospheric fluctuations and instrumental limitations may limit the accuracy of position measurements.

We further discuss below the boundary conditions or requirements in astrometric observations. Table 2 at the end of this section summarizes the limitations with respect to the IRAM array.

### 20.5.1 Known Limitations

Among several practical limitations it is worth mentioning: wind effects, thermal effects in the antenna structure (including de-icing instabilities), the influence of refraction effects, imperfections in subreflector displacements, imperfections in the azimuth and elevation bearings of the antennas and, not least, uncertainties in the "crossing point" of the azimuth and elevation axes. These imperfections, and in fact the resulting differential effects of each antenna pair in the array, have adverse effects on the visibility phase measurements; however, many of them can be removed to a large extent by phase calibration (a posteriori), and thus will not be discussed further.

In order to make the reader more aware of these questions, we just mention that the large-scale uneveness of the azimuth bearings gives rise, in places, to optical path deviations of about 40 $\mu$m which translate into position offsets of $0.04''$ with 200 m baselines. Likewise, position uncertainties result from imperfections in the "crossing point" of the azimuth and elevation (nodal point) of each antenna in the array (see Chapter 6). Slow drifts in the focal position are also corrected to first order by the calibration procedure. Only large and rapid focal drifts are problematic if not recognized as such in the phase of a reference calibrator.

### 20.5.2 Practical Details

We elaborate here on some properties of the IRAM array related to inaccuracies in the determination of baseline lengths, and we briefly discuss how atmospheric phase noise and source strength can limit the accuracy of position measurements.

- **Baselines:** are easily measured with the IRAM interferometer on Plateau de Bure with a precision of a few degrees or a small fraction of one millimetre. As a reference, good winter conditions allow us to measure baselines at 86 GHz, using a number of quasars well-distributed in hour-angle and declination, with uncertainties of $5^\circ - 8^\circ$ in the D configuration (the most compact one at IRAM) and $10^\circ - 20^\circ$ in the A configuration. But even the most accurate baseline measurement will be limited in precision. Residual uncertainties in the baselines will finally produce phase errors that scale with $\Delta\vec{k} = \vec{k}_{\rm quasar} - \vec{k}_{\rm source}$, the distance between a calibration quasar and the source. Combining the different forms of the phase equation defined in Section 20.2, we can then derive a rough estimate of the mean uncertainty in the absolute position of a source from

$$\Delta\theta \simeq (\delta\vec{\mathcal{B}} \cdot \Delta\vec{k})/\mathcal{B} \simeq (\delta\phi/2\pi)\ (\lambda/\mathcal{B}) \simeq (\delta\phi/2\pi)\ \theta_B \tag{20.22}$$

  where $\delta\phi$ is the phase error due to inaccuracies in the baselines. This formula is convenient, as it associates uncertainties in the knowledge of the baseline length at a given frequency with $\theta_B$, the synthesized beam. For instance, observations at 86 GHz in the D configuration with baseline phase residuals $\delta\phi$ between $2^\circ$ and $5^\circ$ (i.e. assuming baseline errors, $\delta\vec{\mathcal{B}} = 0.2$ mm, and typical phase calibrator distances, $\Delta\vec{k} = 5^\circ - 15^\circ$) appear to have position uncertainties smaller than $0.20''$. See Subsection 20.4.2 for suggestions to improve these uncertainties.

- **Atmospheric phase fluctuations** are among the most important limitations that affect the accuracy of position measurements. Poor seeing conditions imply phase decorrelation which in turn implies reduced flux density sensitivity and larger apparent source sizes (see Chapters 9 and 10). When the atmospheric phase noise dominates, phase decorrelation can be estimated by least-square fitting in time the phase profile of a reference calibrator. Under the assumptions made at the end of Section 20.3 or assuming here that the atmospheric phase fluctuations remain unchanged, namely $\sigma_\phi$ is similar for each phase sample, we can estimate the mean angular uncertainty from

$$\Delta\theta \simeq \sigma_\phi/(2\pi\sqrt{n_p}(\mathcal{B}/\lambda)) = \sigma_\phi\,\theta_B/(2\pi\sqrt{n_p}) \tag{20.23}$$

  where $n_p$ is the number of phase samples. The size of the associated "seeing disk" is defined as $(\sigma_\phi/2\pi)\sqrt{8\ln 2}\,\theta_B$. For instance, measuring mean atmospheric phase fluctuations $\sigma_\phi \simeq 10^\circ$ at 86 GHz on a 60 m baseline is equivalent to observe in $\simeq 0.78''$ seeing conditions (which is small since $\theta_B \sim \lambda/\mathcal{B} \sim 12''$ and corresponds to a small fraction of the synthesized beam). Observations at the same

frequency, on the same baseline and with similar atmospheric conditions will then provide a position accuracy of order $\Delta\theta \simeq 0.33''/\sqrt{n_p}$ (or 3% of $\theta_B \sim 12''$).

- **Source strength** and finite signal to noise ratio is another important limitation to astrometric accuracy. While reference calibrators have to provide enough sensitivity for rapid detection, detection of program sources may require hours of integration. In addition, observed sources are sometimes resolved out with extended configurations. Therefore, the interesting astrometric case described in Section 20.4 where spectral sources are rather easily detected may not be common in mm-wave astronomy. As mentioned in Section 20.4.2 we can use the result of [Reid et al. 1988] to estimate the one sigma position uncertainty

$$\Delta\theta = \sigma_\theta \simeq \ (\theta_B/2)(\sigma_S/S) = \theta_B/(2 \cdot \mathrm{SNR}) \tag{20.24}$$

where $\sigma_S$ is the noise in the map and $S$ the source flux density. With the IRAM array in the D configuration, a source at mean declination (e.g. $30° - 40°$) detected with a signal-to-noise SNR $\simeq 5$, cannot be located with a precision better than 10% of $\theta_B$ (e.g. $0.25''$ at 230 GHz). Uncertainties in declination measurements will obviously be larger for southern sources owing to the elongation of the synthesized beam.

On the other hand, astrometric observations of bright sources such as the SiO line sources presented in Section 20.4 are not limited by SNR issues in general, but by the accuracy of the bandpass calibration. While delay calibration (see Chapter 5) already removes the bulk of the phase gradient across the band selected for observations, residual variations can only be removed by observing strong calibrators. Using the classical radiometric equation, bandpass calibration requires the following:

$$\Delta t^C = (S \cdot \sigma_S)^2/(C \cdot \sigma_C)^2 \Delta t^S \tag{20.25}$$

In this expression, $S$ and $C$ are the flux densities of the source and calibrator, $\sigma_S$ and $\sigma_C$ the respective r.m.s. noise levels, and $\Delta t^S$ and $\Delta t^C$ the integration times on the source and calibrator. For instance, a 1 sec integration on a 15 Jy calibrator like 3C273 (at the time of writing, the strongest calibrator at 86 GHz available in the northern sky) is sufficient for bandpass calibration in the case of a $5\sigma-$detection of a 2 mJy source. (In practice, however, several seconds integration would be better.) On the other hand, a 10 min integration on the same calibrator would just be sufficient to meet the minimum requirement ($\sigma_S = \sigma_C$) to calibrate 1 min observations of a 50 Jy strong source.

There are a few other issues which we list below. They are worth mentioning although there is little implication for observations with the IRAM array. (For other effects such as bandwidth smearing and visibility averaging, we recommend reading the book of [Thompson et al. 1986]; see Chapter 6.)

- **Pointing offsets** is a potential source of position errors. Ideally, the phase of the incoming wavefront does not depend on pointing offsets across the Airy (or diffraction) pattern. However, imperfections in the optical system may result in differences in the Airy pattern from an antenna to another in the array (although all antennas are of comparable quality). Experience at 86 GHz shows, that rather strong phase differences (up to 10°) may appear when antennas are individually offset from the target position by a distance equal to half the primary beamwidth (HPBW).

- **Primary beam attenuation** produces a radial displacement for off-axis targets. It needs to be corrected for targets at large angular distances ($\simeq$ HPBW/2) from the phase tracking center of the interferometer.

- **Gravitational Lensing** by the Sun introduces positional offsets $\sim M_\odot/D_E(\sqrt{1+\cos\theta}/\sqrt{1-\cos\theta})$ which are negligible for targets outside the Sun avoidance region of the IRAM antennas ($\theta \geq 45°$). For instance $\Delta\theta \ \simeq 0.1''$ at $\sim 5°$ from the Sun limb.

A summary of the main practical position uncertainties for the IRAM array is given in Table 2 in arc second or in terms of the synthesized beam $\theta_B$; $\mathcal{B}$ is the baseline length in meter. Only instrumental errors are removed to first order by calibration.

**Table 2. Plateau de Bure Interferometer – Main Sources of Position Uncertainty**

| TELESCOPE* | $\Delta\theta$ | Calibration |
|---|---|---|
| Focus Offset | $\leq 0.20'' \cdot (100/\mathcal{B})$ | Yes |
| Axes Non-Intersection | $\leq 0.10'' \cdot (100/\mathcal{B})$ | Yes |
| AzEl Bearings | $\leq 0.08'' \cdot (100/\mathcal{B})$ | Yes |
| OBSERVATION | | |
| Atmospheric Seeing† | $\leq 0.06 \cdot \theta_B$ | No |
| Calibrator Distance† | $\leq 0.02 \cdot \theta_B$ | No |
| Pointing Offset | $\leq 0.02 \cdot \theta_B$ | Partially |
| Source Intensity | $\leq (0.5/\mathrm{SNR}) \cdot \theta_B$ | No |

† Upper limits are illustrative for astrometric observations in limiting conditions. See text for more details.
* Instrumental values are all calibrated out to first order.